Microstructure and tensile properties of tungsten at elevated temperatures

Tielong Shen [a, b], Yong Dai [a, *], Yongjoong Lee [c]

[a] Laboratory for Nuclear Materials, Paul Scherrer Institut, 5232 Villigen PSI, Switzerland
[b] Institute of Modern Physics, Chinese Academy of Sciences, Lanzhou 730000, China
[c] European Spallation Source, Tunavägen 24, 223 63 Lund, Sweden

HIGHLIGHTS

- This work was conducted to support the development of the 5 MW spallation target for the European Spallation Source.
- The effect of fabrication process on microstructure, ductile-to-brittle transition temperature and tensile behaviour was studied with hot-rolled and hot-forged tungsten.
- The tungsten materials were characterized with metallography analysis, hardness measurement and tensile test in a temperature range of 25–500 °C.
- The results indicate that the HR tungsten has better mechanical properties in terms of greater ductility and lower ductile-to-brittle transition temperature.

ARTICLE INFO

ABSTRACT

In order to support the development of the 5 MW spallation target for the European Spallation Source, the effect of fabrication process on microstructure, ductile-to-brittle transition temperature (DBTT), tensile and fracture behaviour of powder-metallurgy pure tungsten materials has been investigated. A hot-rolled (HR) tungsten piece of 12 mm thickness and a hot-forged (HF) piece of about 80 mm thickness were used to simulate the thin and thick blocks in the target. The two tungsten pieces were characterized with metallography analysis, hardness measurement and tensile testing. The HR piece exhibits an anisotropic grain structure with an average size of about $330 \times 140 \times 40$ μm in rolling, long transverse and short transverse (thickness) directions. The HF piece possesses a bimodal grain structure with about $310 \times 170 \times 70$ μm grain size in deformed part and about 25 μm sized grains remained from sintering process. Hardness (HV0.2) of the HR piece is slightly greater than that of the HF one. The ductility of the HR tungsten specimens is greater than that of the HF tungsten. For the HF tungsten piece, specimens with small grains in gauge section manifest lower ductility but higher strength. The DBTT evaluated from the tensile results is 250–300 °C for the HR tungsten and about 350 °C for the HF tungsten.

1. Introduction

Pure tungsten has been widely used as target material at the spallation neutron sources such as LANSCE (Los Alamos Neutron Science Centre) [1,2] and ISIS (neutron source at the Rutherford Appleton Laboratory) [3] and will be applied to the ESS (European Spallation Source) [4] target as well. Due to the high beam power (5 MW), a rotating target has been chosen as the design option at ESS, in order to distribute the beam energy and the radiation damage more uniformly in the spallation volume. Fig. 1 shows the sketch of the ESS target wheel baseline design as of December 2014. The target wheel is 2.58 m in diameter and 11.6 cm in height. The target wheel is divided into 33 segments for structural reasons, and each segment consists of 12 tungsten blocks with varying thicknesses ranging from 12 mm in the beam upstream region with higher volumetric energy deposition to 120 mm in the beam downstream region with reduced heat loads. The tungsten blocks are cooled by helium flow with the mass flow rate 3 kg/s at 1.0 MPa. At 5 MW the operation temperature in the tungsten volume could reach up to 500 °C [4].

* Corresponding author.
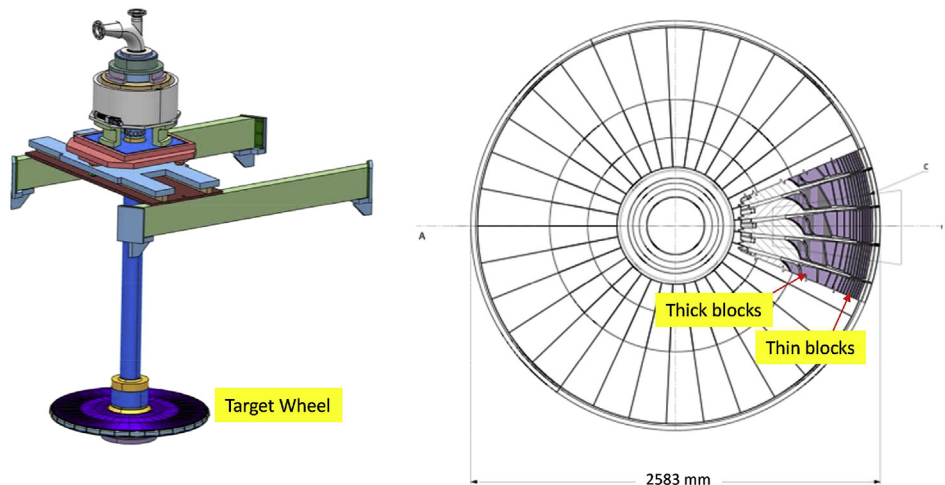E-mail address: yong.dai@psi.ch (Y. Dai).

Fig. 1. The snapshot of the ESS target wheel, the baseline design as of December 2014. The left side shows schematically the target. The right side shows schematically some sections of the tungsten target wheel.

Tungsten is normally powder metallurgy pressed and sintered. To increase the density and improve mechanical properties, sintered tungsten needs to be hot-worked, either by hot-rolling or hot-forging. Compared to hot-forged (HF) tungsten, hot-rolled (HR) tungsten usually possesses higher density and better mechanical properties. However, due to difficulties of hot-rolling processing the thickness of HR tungsten plates is limited to 30—40 mm. Therefore, it is considered to use HR tungsten for the first several plates in each section, where the proton and neutron fluxes and heat deposition are high, while HF tungsten for the rear part where thick plates can be applied.

Properties of tungsten materials may vary greatly from one product to another, depending on production route [5—9]. For this reason, a study of HR and HF tungsten materials is necessary for the robust design of the target. In addition, for the typical target operation temperature range, 50—500 °C, very limited published tensile data could be found for commercially available thick (>10 mm thickness or diameter) tungsten plates or rods [6,10]. It should be pointed out that a lot of research work has been done for fusion applications as described in overview papers like [11,12]. However, the most of the publications are on materials development, for example improving tungsten properties with small amounts (normally < 1%) additions (e.g. Ref. [12]) or developing specific processing routes (e.g. Refs. [13,14]). These are, for the time being, not relevant to the ESS application. For the first ESS target, based on the existing knowledge and experience available for LANSCE and ISIS [1—3], just pure tungsten of normal industrial products has been selected as the target material. Due to a great difference in quality and price of commercially available tungsten materials, products of several companies in Europe and China have been pre-selected. Metallography and mechanical tests have been conducted to characterize the materials of the different companies. The final selection will be made based on the results of the characterization and with a compromise of cost. In this work, HR and HF tungsten materials of a Chinese company, Tianlong Tungsten & Molybdenum Co. Ltd., were studied. Tensile, bend and fatigue specimens were fabricated from several HR and HF tungsten pieces of different thicknesses in the interested range relevant to the ESS target have been tested, for the temperature range from room temperature up to 500 °C. The fatigue test results together with few tensile data were published in Ref. [15]. In this paper the results obtained from extensive tensile tests on the HR tungsten with different orientations and HF tungsten will be reported.

2. Experimental

2.1. Material and specimen preparation

The tungsten materials used in this study were purchased from Tian-long Tungsten & Molybdenum Co., Ltd., Beijing, China. A HR tungsten plate of 12 mm thickness and a HF plate of about 80 mm thickness were used for specimen preparation, as illustrated in Fig. 2. The HR plate was rolled five times at temperatures between 1450 and 1650 °C with a 20—25% thickness reduction each time. The HF piece was forged three times in Z-direction at temperatures between 1550 and 1700 °C with a 20—25% reduction each time, during which it was also pressed slightly in X-direction. Miniature type tensile specimens (Fig. 3) were cut from the HR and HF tungsten plates using an electro-discharge machine (EDM). Because of anisotropic structure induced by hot work processing, two different groups of specimens were cut from the HR plate: Group-A tensile specimens with the tensile axis being parallel to the long-transverse direction (X-axis) and the main surface in the a-plane; Group-B tensile specimens with the tensile axis parallel to the rolling direction (Y-axis) and the main surface in the b-plane (Fig. 2). For specimens of the HF tungsten the tensile axis is perpendicular to the forge direction. After EDM cutting, the specimens were milled to the required thickness of 0.75 mm. In order to study surface effect on mechanical properties of tungsten, a part of the specimens were electro-polished. About 15 microns were removed from surface layer. Fig. 4 presents optical microscopy pictures of specimens in as-milled and electro-polished conditions.

2.2. Metallography observation and hardness measurement

Metallography observation and hardness measurement were performed. The specimens were prepared with fine mechanical polishing and electro-chemical etching at room temperature. The electrolyte was 5% NaOH and 95% H_2O. The microstructural observation was performed with an optical microscope. Most of the images were taken at magnifications of 10 and 20 times. Hardness (HV0.2) was measured with a Vickers hardness tester following ASTM Standard E 92 with 0.2 kg force and 15 s full-loading time. Ten indentations were performed on each measured specimen.
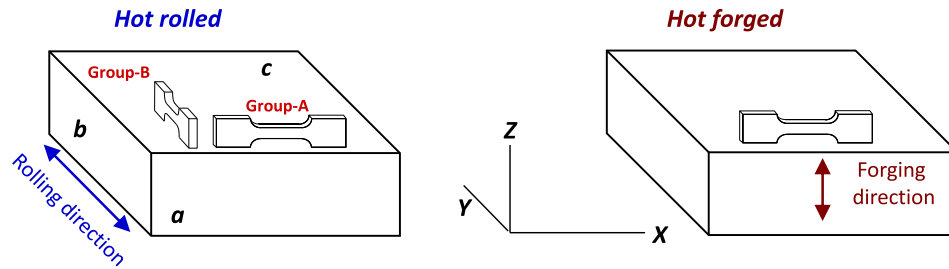
Fig. 2. Sketches showing rolling and forging directions and definition of different planes (*a, b, c*) and directions (*X, Y, Z*) and the orientation of the tensile specimens.

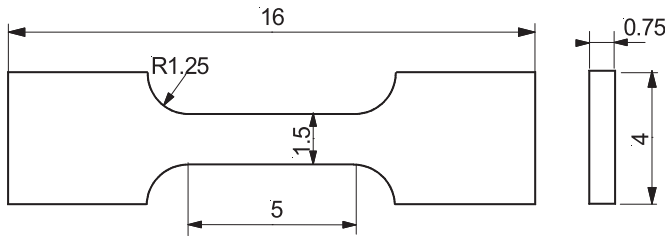**Fig. 3.** Dimensions of the tensile specimen.

2.3. Tensile testing

Tensile tests were conducted using a 2 kN MTS testing machine at a stain rate of 1×10^{-3} s^{-1} in flowing N$_2$ gas. The tests were conducted at room temperature (RT) and elevated temperatures between 150 and 500 °C. The testing machine was equipped with a video-extensometer so that elongation could be measured directly from the gauge section of a specimen. Each test was run until the specimen failed thoroughly. After tensile testing, fracture surfaces of some selected specimens were observed using the scanning electron microscopy (SEM) to identify the fracture modes of the specimens.

3. Results and discussions

3.1. Metallography observation and hardness measurement

The grain structure in the *a*-, *b*- and *c*-planes of the HR tungsten plate is shown in Fig. 5. It looks similar to that of the cross-rolled tungsten plate tested in our previous work [7] but with a larger grain size. Grains are in a "pancake" shape but elongated in the rolling direction (Y-direction) as can be seen by comparing Fig. 5a and b with Fig. 5c. The average grain size is about $140 \times 330 \times 40$ μm in X, Y and Z directions, respectively. The grain

structure of the HF tungsten plate is shown in Fig. 6. The grains are flattened in the forging direction (Z-direction, Fig. 6a) but little more equiaxed on the *c*-plane (Fig. 6b). The average grain size is about $170 \times 310 \times 70$ μm in X, Y and Z directions, respectively. Another feature is the bimodal grain size distribution of the HF tungsten plate (Fig. 6c). A large part of the HF tungsten plate consists of small grains of about 25 μm measured on the *c*-plane, about 10 times smaller than the large ones. In Fig. 6 one can also see a lot of pores located either inside grain matrix or on grain boundaries. The porosity results in a density of 18.93 g/cm^3 for the HF tungsten, namely about 98.3% of the theoretical density of tungsten. The density of the HR tungsten was measured as 19.23 g/cm^3, namely 99.9% of the theoretical density of tungsten.

The result of hardness measurement is presented in Fig. 7. Hardness (HV0.2) was measured on the *a*-, *b*- and *c*-planes of the HR tungsten. The result indicates that the hardness measured on the *b*-plane is slightly higher (about 6%) than that measured on *a*- and *c*-planes. For the HF tungsten, the hardness measured on the *c*-plane is about 10% lower than that measured on *a*- or *b*-plane. The hardness measured in areas with small grains is not much higher than that measured in areas with large grains as shown in the figure. The error bars indicated in the figure were given by ten measurements on each plane. In general the hardness of the HR tungsten material is slightly higher than that of the HF tungsten, 492 ± 15 versus 479 ± 20. The small difference in hardness values measured on different planes may be attributed to inhomogeneity of the materials in terms of localized deformation (hot-work) degree, grain size, grain orientation etc.

3.2. Tensile testing

Tensile results of the HR tungsten material are presented in Fig. 8. Fig. 8a shows the results of the Group-A specimens with tensile axis along the long-transverse direction (X-direction) and Fig. 8b shows the ones for the Group-B specimens with tensile axis along the rolling direction (Y-direction). The solid lines are for as-
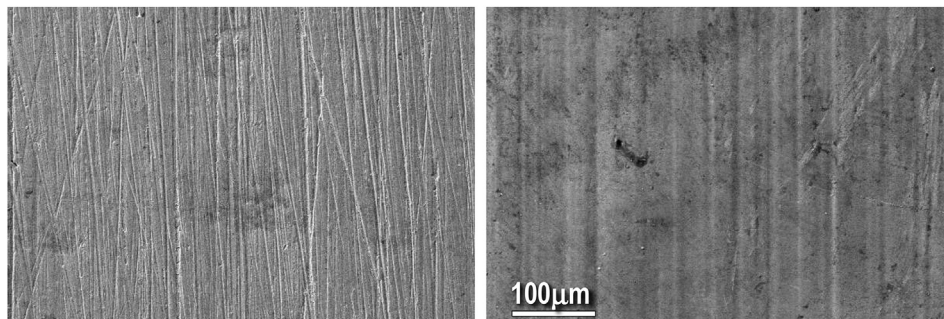

Fig. 4. SEM micrographs showing the surfaces of an as-milled specimen (left) and an. electro-polishing specimen (right) of HR tungsten. The scale indicated is the same for both graphs.
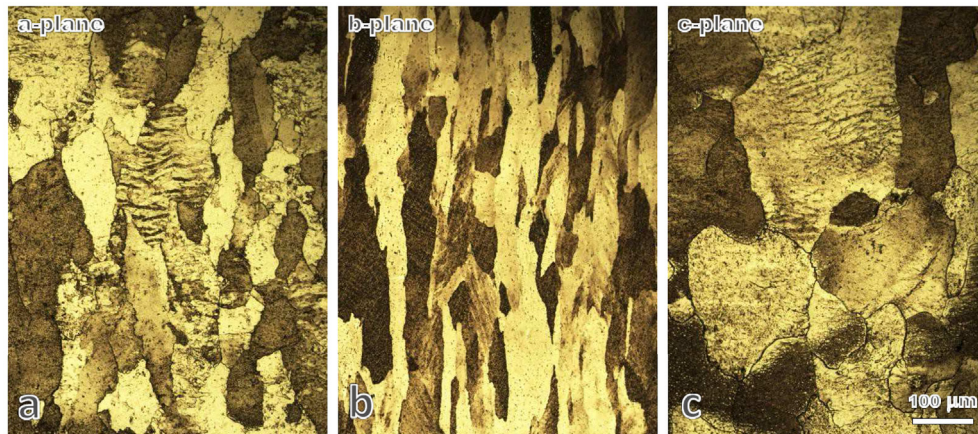
Fig. 5. Typical microstructure observed on different planes of the HR tungsten plate: (a) *a*-plane; (b) *b*-plane; (c) *c*-plane as shown in Fig. 1. The scale indicated is the same for all graphs.
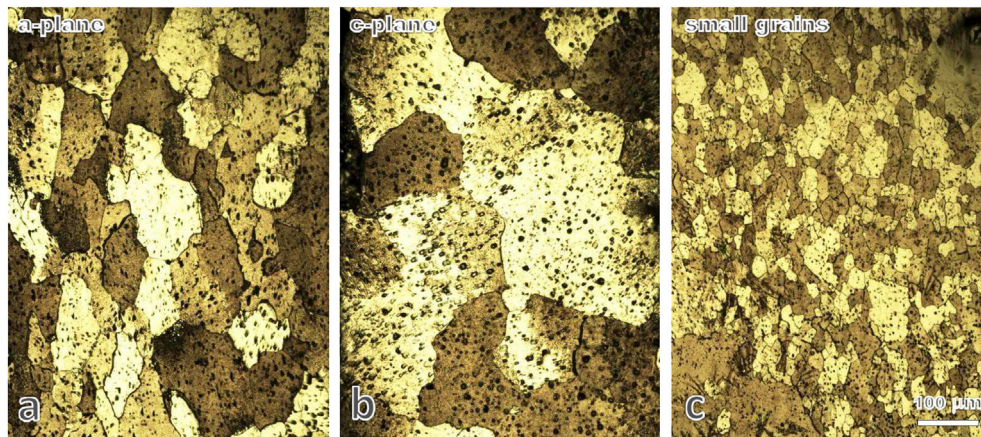

Fig. 6. Typical microstructure observed on different planes of the HF tungsten plate: *a*-plane, *c*-plane; and small grain area of *c*-plane. The scale indicated is the same for all graphs.
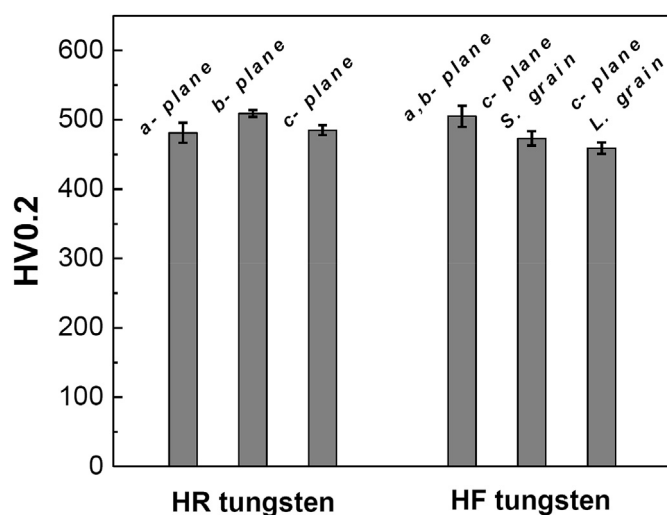

Fig. 7. Hardness measured on different planes of both HR and HF tungsten specimens.

milled (AM) specimens and the dashed lines for electro-polished (EP) specimens. The two groups of specimens show essentially the same strength, particularly at temperatures about 250 °C.

However, on average the Group-B specimens have larger ductility than the Group-A specimens. At temperatures up to 200 °C both groups of specimens failed in elastic regime or at very low plastic deformation level. At 250 °C the ductility of the Group-B specimens was starting to recover, while ductility of the Group-A specimens was still very low. At 300 °C the Group-B specimens became nearly fully ductile, whereas the Group-A specimens demonstrated a situation similar to that of the Group-B specimens at 250 °C. This indicates that the ductile-to-brittle transition temperature of Group-B specimens is about 50 °C lower than that of the Group-A specimens. The difference in ductility of the two groups of specimens could be attributed to grain orientation effect, because crack propagation along rolling direction is easier, as observed by Noto et al. on hot-rolled or extruded tungsten [9].

Comparing the tensile results of the as-milled specimens with that of the electro-polished specimens, it can be seen that the electro-polished surface condition did not show any clear influence on the tensile properties of both groups of specimens. This is in agreement with our previous results obtained from 3-point bend testing on smooth specimens [7], which did not show any clear effects of electro-polishing on the flexure strength of the bend specimens.

Fig. 9 presents the results of the HF tungsten specimens tested at the same temperatures between RT and 500 °C. It can be seen that the tensile results look quite similar to that of Group-A HR
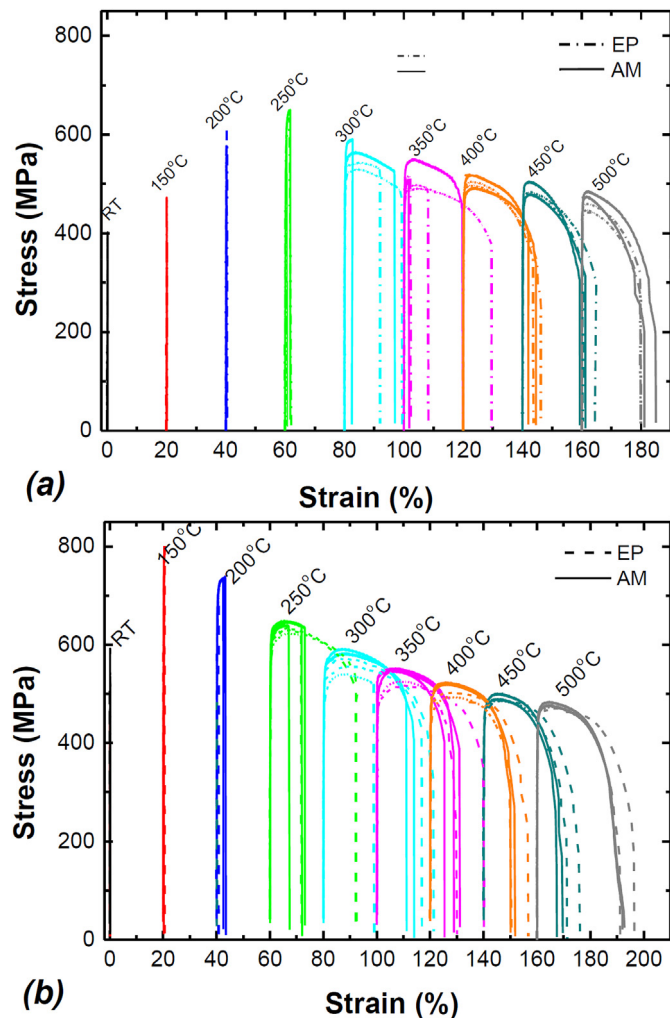
Fig. 8. Tensile stress–strain curves of the HR tungsten specimens tested in a temperature range of 25–500 °C: (a) Group-A specimens with tensile axis along the long-transverse direction and (b) Group-B specimens with tensile axis along the rolling direction.
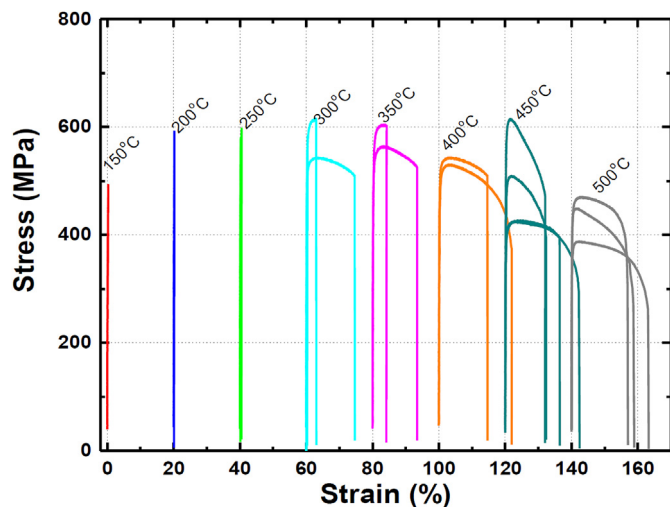

Fig. 9. Tensile curves of the HF tungsten specimens tested in a temperature range 150–500 °C.

specimens, but with slightly larger scatter. The larger scatter could be attributed to the bimodal grain size structure. It was found that the three specimens tested at 450 °C were of different grain structures. The one with the highest strength had small grains (Fig. 6c) in the gauge section, while the one with lowest strength had large grains (Fig. 6b).

The dependence of test temperature of tensile properties for the HR and HF tungsten materials is shown in Fig. 10. As for strength, it was expected that the HR tungsten should be higher due to a higher degree of hot-deformation (5 deformation steps vs 3 steps for the HF tungsten) [5]. However both materials have nearly the same strength at temperatures above 250 °C. At ≤250 °C the strength (fracture stress) of the HF tungsten is lower, although both materials are brittle. The difference in the ductility is evident. In the ductile regime, the HR tungsten specimens exhibit nearly 50% higher ductility as compared to the HF tungsten specimens. It can be clearly seen that the transition of ductile to brittle regime takes place around 250 °C for the HR tungsten and about 350 °C for the HF tungsten. This could be attributed to the higher deformation degree of the HR tungsten, because normally hot-deformation increases ductility and fracture toughness of tungsten [5,8].

As previously mentioned tensile data of thick tungsten plates or rods are very limited, particularly at lower temperatures below
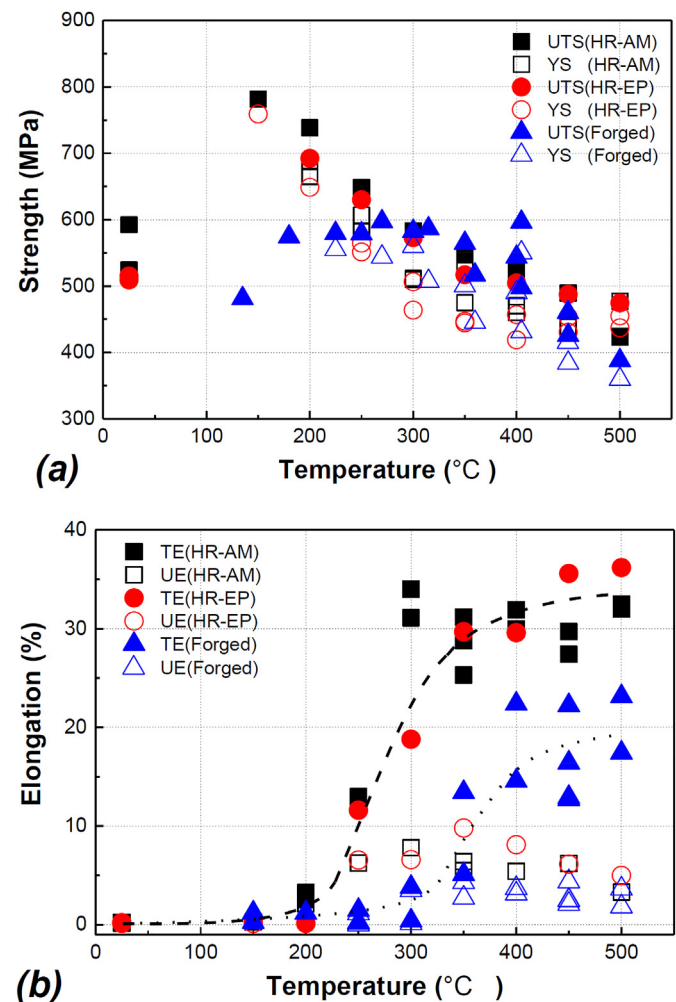

Fig. 10. Test temperature dependence of (a) yield strength (YS) and ultimate tensile strength (UTS) and (b) uniform elongation (UE) and total elongation (TE) for the HR tungsten Group-B specimens in as-milled (AM) and electro-polished (EP) surface conditions and the HF tungsten specimens in as-milled surface condition.
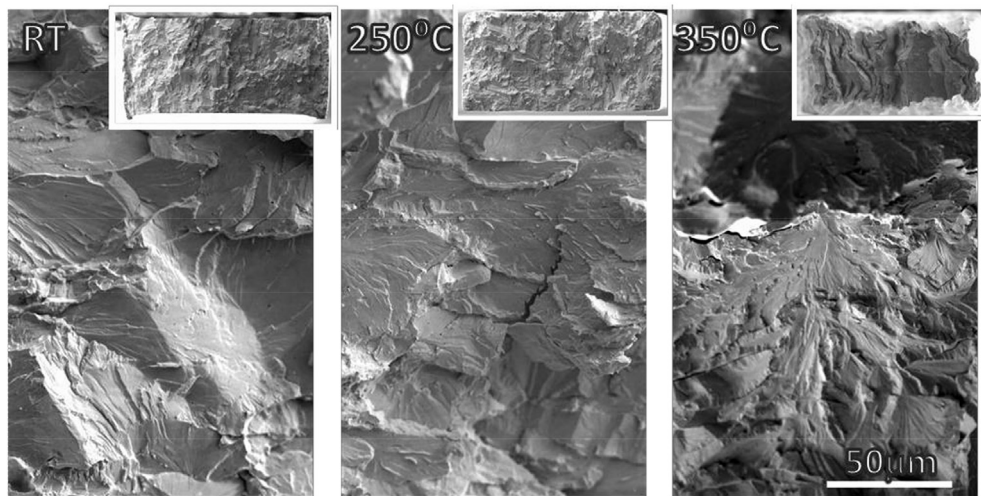
Fig. 11. SEM micrographs showing fracture surfaces of HR tungsten specimens tested at different temperatures: RT, 250 and 350 °C. The scale indicated is the same for all graphs.

500 °C. Nevertheless, some tensile data obtained by Noto et al. [9] from a 12 mm thick rolled tungsten plate (produced by A.L.M.T. Corp.) for the ITER diverter application are comparable with the present results. The yield stress values, about 620 MPa at 200 °C and 420 MPa at 400 °C, are in the same range of that shown in Fig. 10.

Compared with the preliminary tensile data obtained from a 20 mm thick plate of the same batch of tungsten and with larger tensile specimens [14], the present results show similar strength but greater elongation values. This is in agreement with general observations of tungsten materials. Thinner tungsten pieces are easier to introduce hot-deformation to improve the mechanical properties.

3.3. SEM observation

Some specimens were selected for SEM observation to identify the fracture behaviour of the specimens. In Group-B specimens of the HR tungsten, specimens tested at RT, 250 and 350 °C were selected as representatives for specimens failed in brittle, transition and ductile regime. For the HF tungsten specimens, ones tested at 300, 400 and 500 °C were used as representatives for specimens failed in brittle, transition and ductile regime.

The appearance of the fracture surface of the three HR specimens is presented in Fig. 11. The fracture mode is transgranular cleavage type for all the three specimens. However, a great difference between the brittle and ductile fracture was observed. The specimen tested at RT and failed in brittle manner did not show any necking, while the one tested at 350 °C and failed in ductile manner exhibited strong necking and with coarse secondary cracks on the fracture surface. The situation of the one broken in the transition region was between the brittle and ductile cases. Slight necking and fine secondary cracks were detected.

The fracture appearance of the HF specimens (Fig. 12) was little different from that of the HR specimens, although some common features were observed. For the specimen tested at 300 °C, a mixed type of cleavage and intergranular fracture appeared. In the transition region, brittle intergranular fracture was also seen, although the specimen exhibited some ductility. It is interesting to note that the intergranular fracture mainly happened in the small grain region as can be seen in the figure. However at 500 °C the specimen was very ductile. Not only strong necking but also large secondary
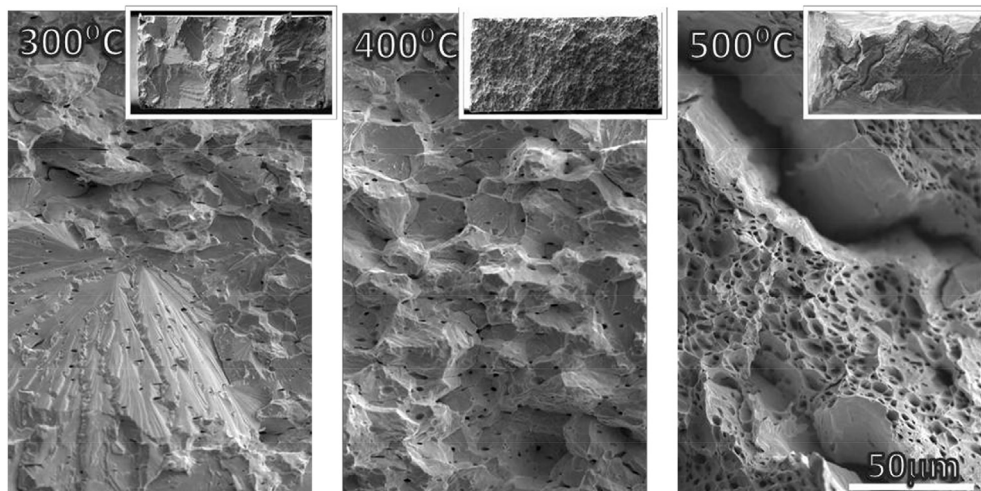

Fig. 12. SEM micrographs showing fracture surfaces of HF specimen tested at different temperatures: RT, 250 and 350 °C. The scale indicated is the same for all graphs.

cracks and large dimples appeared on the fracture surface.

The observation indicates that a process ensuring thorough hot deformation is essential for a HF tungsten piece. Otherwise the original grain structure from previous sintering process may remain in some part of the forged piece, which is more brittle than the deformed part as indicated by the tensile results (Fig. 9). This means some additional hot forging may be required.

4. Conclusions

In order to support the development of the ESS spallation target, HR and HF tungsten materials have been investigated. The materials were fabricated according to the thin and thick blocks in the target (preliminary design). The grain structure was inspected with metallography observation. Tensile properties of the materials were obtained by tensile testing at temperatures up to 500 °C. Conclusions drawn from the results are as follows:

1. The HF tungsten piece, due to its great thickness, has a bimodal grain structure with large grains in hot-deformed part and small grains remained from sintering process. Specimens with small grains in gauge section manifest lower ductility but higher strength. Some additional hot forging is needed to improve the HF tungsten piece.
2. The ductility of the HR tungsten is greater than that of the HF tungsten.
3. The DBTT evaluated from the tensile results is 250–300 °C for the HR tungsten and about 350 °C for the HF tungsten.

References

[1] A.T. Nelson, J.A. O'Toole, R.A. Valicenti, S.A. Maloy, J. Nucl. Mater. 431 (2012) 172.
[2] S.A. Maloy, R.S. Lillard, W.F. Sommer, D.P. Butt, F.D. Gac, G.J. Willcutt, M.R. Louthan, J. Nucl. Mater 431 (2012) 140.
[3] T. Broome, in: F. Carsughi, L.K. Mansur, W.F. Sommer, H. Ullmaier (Eds.), Proc. 2nd Inter. Workshop on Spallation Materials Technology, 1997, p. 55. Ancona, Italy.
[4] ESS-doc-274, ESS Technical Design Report, April 23, 2013. ISBN 978-91-980173-2-8, http://europeanspallationsource.se/documentation/tdr.pdf.
[5] W. Martienssen, H. Warlimont (Eds.), Springer Handbook "Condensed Matter and Materials Data", 2005, p. 303. ISBN 3-540-44376-2.
[6] AFCI Materials Handbook "Materials Data for Particle Accelerator Applications", Rev, vol. 5, Design Properties of Tungsten, 2006 (Chapter 7).
[7] V. Krsjak, S.H. Wei, S. Antusch, Y. Dai, J. Nucl. Mater 450 (2014) 81.
[8] V.I. Trefilov, Y.V. Milman, Proc. 12th Plansee Seminar, vol. 1, Plansee AG, Reutte, 1989, p. 107.
[9] H. Noto, S. Taniguchi, H. Kurishita, S. Matsuo, T. Takashi, J. Nucl. Mater 455 (2014) 475.
[10] K.J. Leonard, in: R.J.M. Konings (Ed.), Chapter 4.06: Radiation Effects in Refractory Metals and Alloys, in "Comprehensive Nuclear Materials", Elsevier Ltd, 2012.
[11] M. Rieth, S.L. Dudarev, et al., J. Nucl. Mater 432 (2013) 482.
[12] H. Kurishita, H. Arakawa, et al., Mater. Trans. 54 (No. 4) (2013) 456.
[13] S. Antusch, L. Commin, J. Heneka, V. Piotter, K. Plewa, H. Walter, Fusion Eng. Des. 86 (2011) 1575–1578.
[14] R. Liu, Z.M. Xie, T. Hao, Y. Zhou, X.P. Wang, Q.F. Fang, C.S. Liu, J. Nucl. Mater 451 (2014) 35.
[15] J. Habainy, S. Iyengar, Y. Lee, Y. Dai, J. Nucl. Mater 465 (2015) 438.